

**Appendix M**  
**Detailed Properties of the Tectorial Membrane**  
**James T. Fulton, [jtfulton@cox.net](mailto:jtfulton@cox.net)**  
**September 6, 2008**  
**Updated February, 15, 2012**

**M.1 Introduction & Overview**

Research related to the mechanics of the cochlea have begun to focus on the tectorial membrane (TM) as a major functional participant in the operation of the Organ of Corti. This focus requires a concise description of the properties of the tectorial membrane in sufficient detail to guide the experimental investigations currently ongoing or planned. That is the goal of this paper. The scope of this paper is limited to the mammalian cochlea unless specifically noted. However, much of the available data has been acquired from other species.

The purpose of this appendix is to focus on the properties required of the TM by the theory of this work and measured values for the TM and its individual elements from the laboratory. A goal is to discuss the properties and performance of the TM in a manner that is consistent with the contiguous nature of the hearing process and the various processes used to achieve its overall performance.

The tectorial membrane is extremely sensitive to its physical environment and is frequently damaged in the process of exposing it for careful analysis. As a result, the majority of the graphical descriptions of the tectorial membrane employ free hand caricatures rather than imagery. These caricatures seldom agree at the detailed level.

The following material will provide a description of the TM in accordance with the theory presented in **Section M.1.1**.

**Figure M.1.1-1**, modified from Lim, will be taken as a gross representation of the Organ of Corti within its active region. The TM is described as an acellular liquid-crystalline structure with a complex internal molecular structure dominated by a few types of proteins in an environment consisting of over 95% water. The structure is essentially transparent in visual light.

## 2 Hearing: A 21<sup>st</sup> Century Paradigm

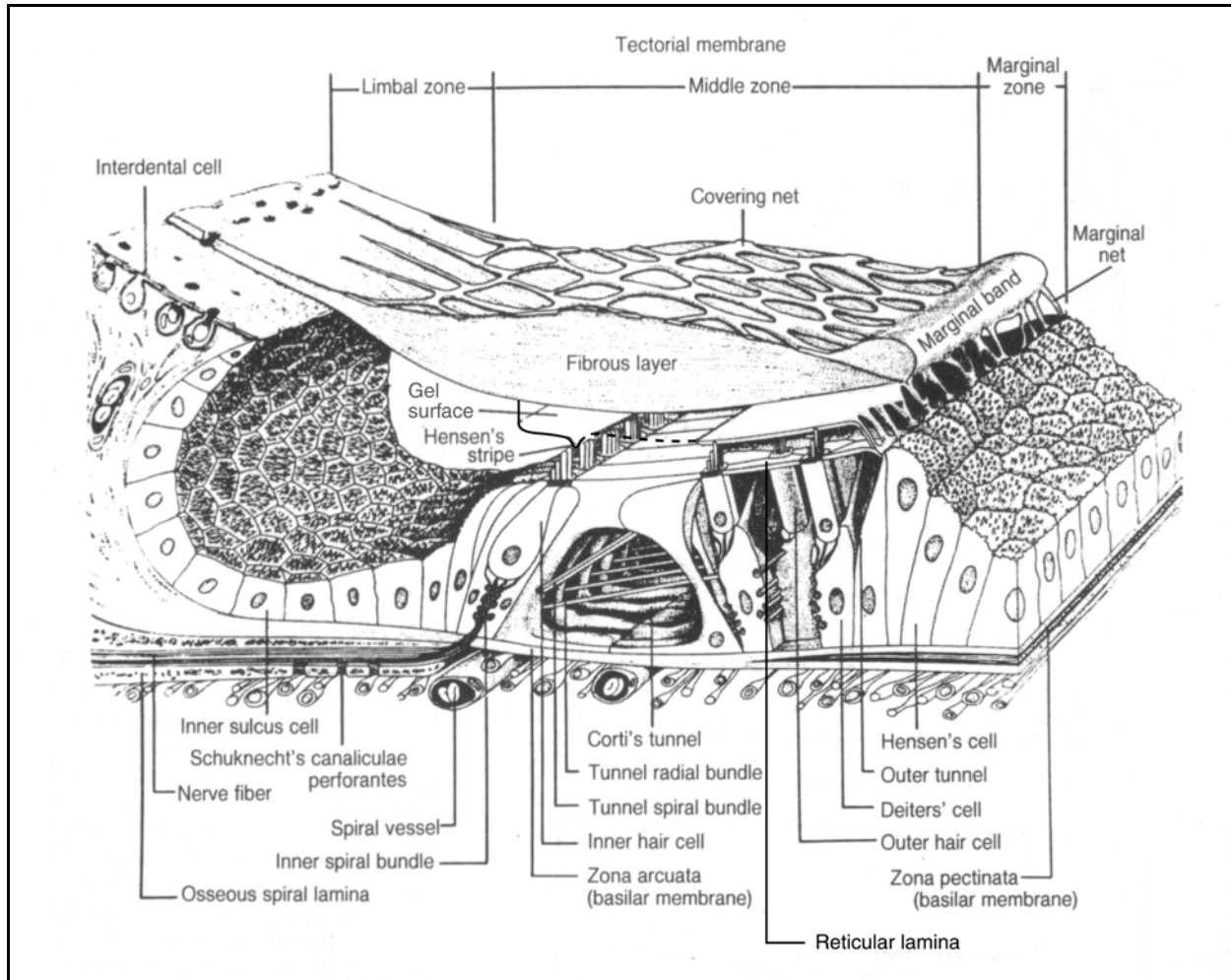


**Figure M.1.1-1** Cross section of the Organ of Corti taken as a gross reference. The lower surface of the TM in the active region is a liquid crystal (colloquially described as a gel surface) generally described as Kimura's membrane. This liquid-crystalline coating on the underside of the fibrous layer of the tectorial membrane has been cut away to show the inner hair cells. The callout's to this coating obscure the total cross sectional area of the spiral tunnel on the left. The structural attachment of the TM to the limbus on the left is generally taken as tenuous. Modified from Lim in Allen, 1992.

Most of the recent experimental investigations have employed mice. The Organ of Corti in the mouse is about 8 mm long compared to 35-38 mm in human. The very small scale of the Organ of Corti as well as the complete labyrinth, makes it difficult to examine their tectorial membrane in detail over its full length. To provide a more complete description of the Tectorial membrane over its full length, **Figure M.1.1-2** from Anson will be used. This figure shows the complete scala media of the human with cross-sections attempting to describe the liquid-crystalline surface of the TM at critical locations.

Inset I shows the proposed cross-section of the liquid crystalline portion of the TM that extends into the vestibular caecum. This structure will be described further below in its role as the surface acoustic wave launcher used to create a slow surface acoustic wave of the Rayleigh type. The shading represents the acoustic energy shown accumulating on the opposite side of the liquid-crystalline layer from the oval window.

Inset II shows the cross-section of the liquid-crystalline portion of the TM as it travels toward the Organ of Corti but before, the cochlear partition begins its in-plane spiral that causes the dispersal of the acoustic energy as a function of frequency. The acoustic energy is shown accumulating on the surface of the liquid-crystalline layer in the vicinity of where the sensory neurons will be encountered farther along the scala media.

Insert III shows the cross-section of the liquid-crystalline portion of the TM within the active region of the Organ of Corti. The acoustic energy has been accumulated within the topographic waveguide known as Hensen's stripe prior to its frequency selective (place-dependent) dispersion.

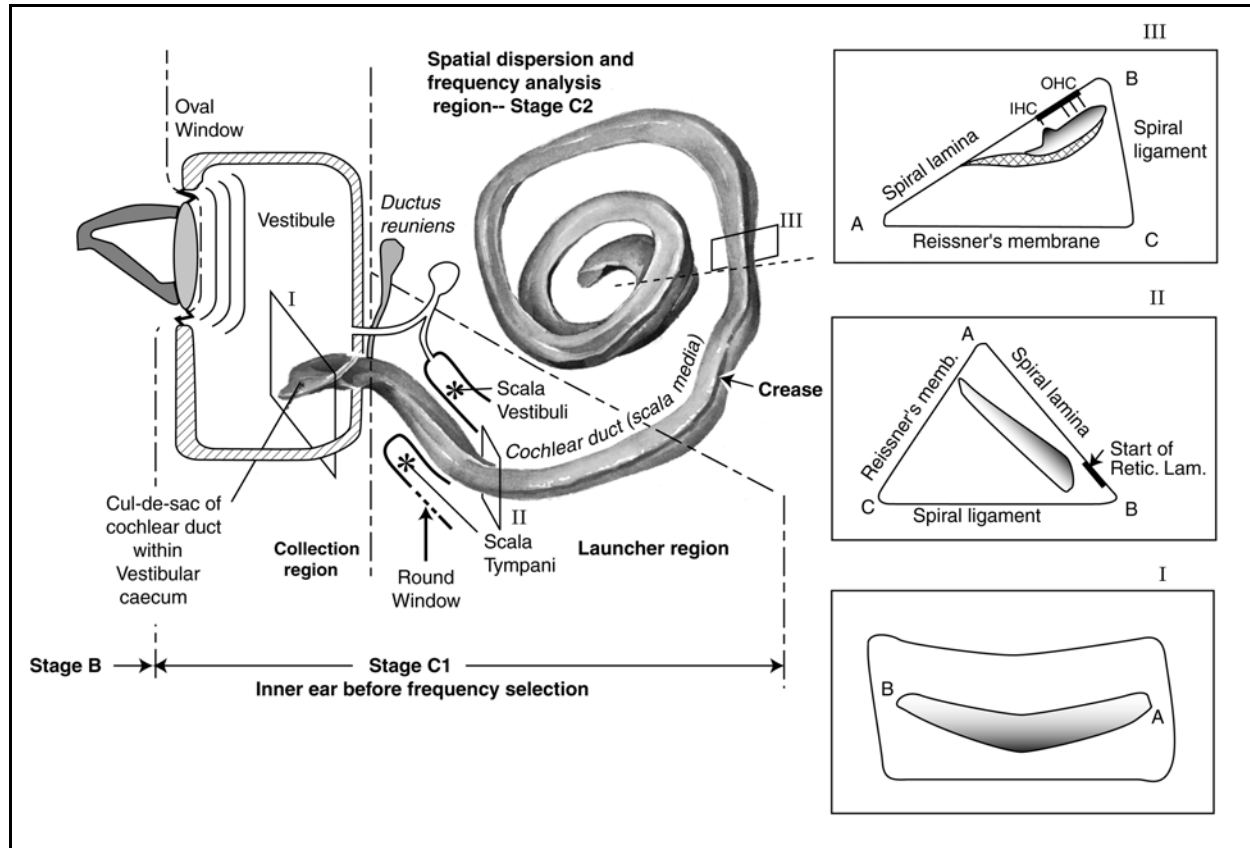


**Figure M.1.1-2** Proposed detail configuration of the vestibule and cochlear duct. Inset I; gel surface of tectorial membrane is the only identifiable feature within the duct. Acoustic energy enters the duct from the top. The gel acts as a large area ( $\sim 1 \text{ mm}^2$ ) second surface SAW launcher. Energy begins to accumulate at the apex of the convex (parabolic) surface. Inset II; the initial section of the cochlear duct twists to maintain a minimum in-plane curvature of the duct while condensing the energy into an area near the future Organ of Corti. The walls of the duct are shown with their eventual labels. They may not be appropriate at this location. Inset III, the gel surface achieves its final shape and location. It is now associated with the remainder of the tectorial membrane acting as an inertial mass. The energy has been concentrated in Hensen's stripe above the IHC. The limited region between the spiral lamina and the spiral ligament forming the basilar membrane is shown by the heavy line. Main figure expanded from Anson, 1992.

### M.1.1 Framework for subsequent discussion

The purpose of this paper is to develop guidelines for future experimentation based on the detailed contiguous model of the hearing process developed from previous experimentation (the essence of the scientific method). This contiguous model has been defined in detail in the chapters of the text, "Hearing: A 21<sup>st</sup> Century Paradigm." The following paragraphs will provide a brief synopsis of the functioning of those parts of the cochlear partition associated with the frequency selective process.

Within the cochlear partition, this model proposes acoustic energy propagates longitudinally along Hensen's stripe subject to a frequency selective mechanism (Marcatili's mechanism) that causes acoustic energy of a specific frequency to be *refracted* out of Hensen's stripe at a specific place. The energy then propagates across the surface of Kimura's membrane until it encounters specific groups of outer hair cells (OHC) where the energy is absorbed and converted to an electrical signal within those sensory neurons.

The employment of the Marcatili mechanism to disperse the frequencies of the acoustic spectrum by refraction,

## 4 Hearing: A 21<sup>st</sup> Century Paradigm

rather than by forced excitation of resonant structures by an undocumented slow traveling wave within the BM, changes the anticipated physical parameters of the relevant materials drastically. Wherein the forced excitation of resonant structures calls for unattainable isolation of adjacent structures at the micron scale, the propagation of a surface acoustic wave along a liquid crystalline surface calls for high coupling between adjacent elements at the same scale in order to achieve very low attenuation losses, and related phase shifts, over distances measured in millimeters.

Understanding the acoustic performance of the tectorial membrane is enhanced by its division into four or more acoustically distinct (heterogeneous) regions (see **Figure M.1.1-1**). The first is Kimura's membrane (including Hensen's stripe) acting as an acellular medium capable of propagating slow surface acoustic waves of the Rayleigh type at a low velocity approximating the Rayleigh velocity for that material. The second is the bulk of the tectorial membrane acting as an inertial mass supporting the efficient transfer of acoustic energy from the surface acoustic waves propagating along Kimura's membrane to the cilia of (both the OHC and IHC) sensory neurons. The third is the specialized areas of the tectorial membrane designed as acoustic channel stops (absorbers). These areas are characterized by the covering net on the side of the TM farthest from the cilia of the sensory neurons and the marginal band and marginal net at the edge of the tectorial membrane farthest from the limbus. The fourth is the specialized lenticular structure embedded in the bulk of the TM nearest Kimura's membrane and apparently acting as a guiding structure to aid the propagation of acoustic energy across the surface of Kimura's membrane and minimizing the spatial spreading of that energy.

The basilar membrane (BM) is not considered an active component in this interpretation of the cochlear partition. It is considered an inertial mass like the bulk of the TM. As a result, the TM and BM move in phase opposition to each other as demonstrated in the laboratory.

As widely noted, the TM consists of over 95% water by weight and/or volume. However, it does not consist of water in the fluid state. The TM is primarily liquid-crystalline in character. The liquid-crystalline state of matter confers upon the TM unique properties that are critically important to its operation. Kimura's membrane in particular consists of a liquid-crystalline structure formed of micelles of protein forming either a face-centered or a body-centered super lattice within a water matrix. This lattice exhibits the properties of a solid at acoustic frequencies above a critical value while acting as a liquid at lower frequencies. As an example, the measured viscosity of this super lattice is greater than 200 Pa•s at audio frequencies while its viscosity at zero frequency is that of water.

The negligible viscosity of Kimura's membrane, at zero frequency makes it very difficult to obtain the detailed physical dimensions of the TM.

To understand the operation of the frequency selective process, it is important that the geometry of the TM be understood to accuracies on the order of  $\pm 1$  micron and angles of  $\pm$  one degree or smaller. This is very difficult to achieve when dealing with liquid-crystalline materials that are extremely sensitive to annihilation through attack by detergents and alkali materials (particularly ionized sodium).

### M.1.1.1 Laboratory techniques of special interest

[Reserved]

### M.1.1.2 Terminology

#### Crystallographic notation

The term centrosymmetric, as generally used in crystallography, refers to a space group which contains an inversion center as one of its symmetry elements. In such a space group, for every point (x, y, z) in the unit cell there is an indistinguishable point (-x, -y, -z). Crystals with an inversion center cannot display certain properties, such as the piezoelectric effect.

Space groups lacking an inversion center (non-centrosymmetric) are further divided into polar and chiral types. A chiral space group is one without any rotoinversion symmetry elements. Rotoinversion (also called an 'inversion axis') is rotation followed by inversion; for example, a mirror reflection corresponds to a two-fold rotoinversion. Chiral space groups must therefore only contain (purely) rotational and translational symmetry. These arise from the crystal point groups 1, 2, 3, 4, 6, 222, 422, 622, 32, 23, and 432. Chiral molecules such as proteins crystallize in chiral space groups.

The term polar is often used for those space groups which are neither centrosymmetric nor chiral. However, the term is more correctly used for any space group containing a unique anisotropic axis. These occur in crystal point groups 1, 2, 3, 4, 6, m, mm2, 3 m, 4 mm, and 6 mm. Thus some chiral space groups are also polar.

## M.2 Detailed description of the tectorial membrane

It is proposed the in-plane curvature of the liquid-crystalline surface of the TM is critically important to the operation of the TM. Describing the function of the liquid crystalline surface of the TM requires detailed knowledge of the local radius of curvature of Hensen's stripe ( $\pm 1$  degree) and the related spatial coordinates of the Outer Hair Cells ( $\pm$  one micron). A particular problem arises in discussing the coordinates of the tectorial membrane and its constituents. A local custom has arisen of using a cartographic coordinate system when viewing the TM. The x-axis of this coordinate system is commonly labeled the longitudinal axis and the y-axis is commonly labeled the radial axis, even though these axes are not related to the structure of the TM itself. As shown in figure 1 of Gueta, Tal et al., reproduced as **Figure M.2.1-1**, the longitudinal axis of the main body (MB), or active portion of the tectorial membrane between the outer hair cell zone (HC) and the limbal region is skewed approximately 15 degrees from the cartographic x-axis. Similarly, the local radius of the transition between the limbal region and the main body differs from the y-axis by about 15 degrees on average. It should also be noted that the axes of the micelles of protein (M) seen radiating from the limbal region of the tectorial membrane differ from the local radius by between 22 and 30 degrees and point toward the apical region as they leave the limbal region defined by Hensen's stripe. A similar situation is seen in figure one of Ghaffari, Aranyosi & Freeman<sup>1</sup>,

### M.2.1 The physical properties of the static tectorial membrane ca. 2006

The liquid-crystalline surface (facing the sensory neurons) of the tectorial membrane is entirely different from the surface facing Reissner's membrane that is covered by a net matrix. The liquid-crystalline face of the tectorial membrane exhibits unique dynamic properties that are critically important to the physiological operation of hearing. These characteristics are presented in Chapter 4. Only the static properties of the tectorial membrane will be addressed in this section.

The tectorial membrane is an element of complex shape and interior construction. It cannot be considered homogeneous for the purposes of hearing theory. The surface facing the scala media is frequently described as having a net like covering. Below this net is a relatively thick material that is heterogeneous at the molecular level and shows a poorly organized structure at larger scales. The protein material in this volume is coiled and cross-linked. The surface of the material facing the reticular lamina consists of a highly organized array of parallel protein molecules that are not coiled or cross-linked. This surface appears to consist of only one layer of protein fibrils. This surface is in turn covered with a liquid-crystalline material that can support a surface acoustic wave.

Iurato has provided some early data on the tectorial membrane and a bibliography<sup>2</sup>. He begins, "The opinions on the structure of the tectorial membrane are manifold and contradictory." Except for values for the bulk physical parameters, and the electron microscope imagery in Iurato, most of the writings prior to 1978 can be disregarded. The relevant work begins with the description of the physical structure of the tectorial membrane of Kronester-Frei<sup>3,4</sup>. Pack & Slepecky have reported on the molecular differences between the forms of tubulin found within the microtubules of sensory neurons<sup>5</sup>. This same material is

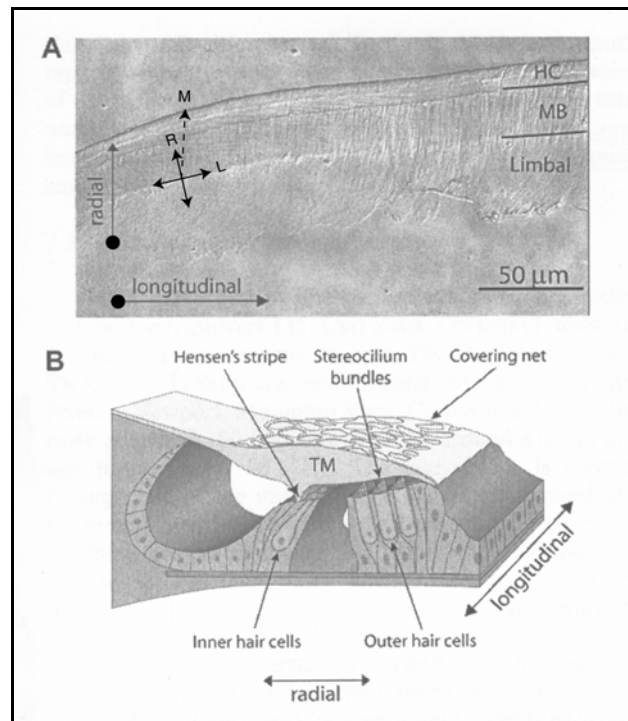


**Figure M.2.1-1** A phase contrast transmitted light microscope image of a TM sample isolated from the basal region. Modified to show the local sample coordinates (double headed arrows) as well as the microscope coordinates. From Gueta, Tal et al., 2007.

## 6 Hearing: A 21<sup>st</sup> Century Paradigm

found in the fine structure of the tectorial membrane. They have stressed that “to understand how sound is processed in the cochlea, an understanding of the cellular differences along its length is crucial, and studying differential protein expression is vital to that understanding.” Both Harrison & Hunter-Duvar<sup>6</sup> and Santi have also provided excellent imagery of the tectorial membrane<sup>7</sup>. The Harrison & Hunter-Duvar image of Hensen’s Stripe in context is particularly valuable.

Kronester-Frei has provided excellent electron micrographs showing that the molecular structure underneath the liquid-crystalline surface of the tectorial membrane varies considerably over its area. The surface of this substrate is remarkably uniform and consists of a structured array of protofibrils with a periodicity of 70 Angstrom and diameters of 110 Angstrom. The axis of the fibrils are arranged at a specific angle of about 71 degrees relative to the unconstrained edge of the TM and point toward the apex of the cochlea. This is a very important characteristic of the substrate. As noted by Novoselova, the curvature of the individual protofibrils is negligible from a structural perspective<sup>8</sup>. The most comprehensive electron micrographs of the “underside” of the tectorial membrane appear to be in Harrison (page 17). However, the precise method of preparation is not described and it is not clear whether the liquid-crystalline coating remained on the specimen. Some of the ribs shown may be the structure underlying the coating.

Along with the very low surface tension noted for the active surface of the tectorial membrane, it can be considered a flat, long, anisotropic plate. The indentations in the uniform area due to the OHCs can be seen by the discerning eye. The character of the surface changes abruptly at Hensen’s stripe and shows ridges parallel to the edge in the region between Hensen’s stripe and the attachment point of the TM at the limbus. The protofibrils in this area are described as type B, consisting of coiled and branched glycoproteins with diameters of 150-200 Angstrom. A similar change occurs in the region Kronester-Frei labels the marginal zone beyond the point of contact of the dendrites of the OHCs. Her figure 5c shows the transition from the protofibrils of the middle zone to the protofibrils of the marginal zone.

Kronester-Frei noted the significant changes (swelling by a factor of two) in the morphology of the TM when the fluids surrounding the element were changed, as has usually occurred during *in-vitro* experiments. The swelling is frequently noted in the literature. The swelling is due to the perilymph attacking the liquid-crystalline surface of the tectorial membrane. This phenomenon probably accounts for much of the inconsistency in the literature concerning the precise dimensions of the TM.

Maskaki et al. have recently provided stress-strain data orally related to the tectorial membrane in a set of knockout mice<sup>9</sup>. Their data suggests the presence of two different materials in the composition of the tectorial membrane. Although they did not claim the tectorial membrane consisted of two separate layers, they did suggest it was heterogenous based on their data. They noted the data suggested that one of the materials had a static stiffness approaching zero (the characteristic of a perfect liquid-crystalline gel). The presence of two materials is further supported by the comments in Cotancke & Corwin. They suggest two separate cellular sources for the protein material and the gel material<sup>10</sup>. The surface tension of the liquid-crystalline coating is extremely low and is known to exhibit unusual features. Radiman et al. have reported on these features in a similar man-made material<sup>11</sup>. They described their material as a clear highly viscous bilayer exhibiting liquid-crystalline structure with a well-defined periodicity. They reported “ringing” that was within the human audible range. Referring to their gels, “(i. e. they ring like a bell when tapped gently) a feature which seems to be associated with the presence of underdamped transverse phonon modes in these systems.” The material was highly sensitive to temperature and tended to become resonant at temperatures near 20 Celsius depending on the level of hydration. At lower levels of hydration, they observed relatively uniform properties over an acoustic frequency range spanning three decades. The investigators exhibited surprise that the material did not show a real elastic modulus at zero frequency. This lack of a modulus at this frequency confirms the liquid-crystalline nature of their material. Many authors have suggested the use of a soft hammer to cause ringing, probably to suppress the generation of higher harmonics in the material.

They noted the change in character with hydration is associated with the transition from a liquid-crystalline to a solid-crystalline behavior. Their conclusion was “Linear rheology confirms that dissipation at high (audible) frequencies is very low and is consistent with the phenomenon of ‘ringing’ in which shear modes in the gel couple to sound via the gel surface.”

### M.2.2 The 3D structure of the tectorial membrane in 2007

Gueta, Tal et al. have recently employed a second harmonic imaging microscope (SHIM) to study the detailed structure of the TM at resolutions achievable with visible light<sup>12</sup>. **Figure M.2.2-1** shows their reconstruction of the apical region of the TM closest to the BM. It shows a stiffer structure forming a shell between the bulk of the TM and the adjacent endolymph. In other literature, this shell is described as Kimura’s membrane. It appears to be on the order of 2-3 microns thick based on the scales in other figures in the paper. Its detailed shape and structure are

beyond the resolution of the data set.

**Figure M.2.2-2** shows their representation of the TM at two locations along the mouse cochlear partition. Gueta, Tal et al. did not give the specific coordinates of the two caricatures in the figure relative to the original TM. It is likely, based on the human mold replica in (**Figure M.1.1-2**) that frame A corresponds to the cross-section II in that figure. This cross-section represents the TM in the non-frequency-dispersive area described as stage C1 in that figure. If correct, the OHC and IHC would not be present in frame A. Similarly, it is likely that frame B corresponds to cross-section III, describing the dispersive stage C2, in the referenced figure. In that case, Kimura's membrane should be shown explicitly or is present as the lower-most layer of the edge of the TM facing the sensory neurons.

### M.2.3 Modes of oscillation within, and on, the TM

The liquid-crystalline character of the TM makes it capable of supporting a variety of acoustic propagation modes. The dominant mode is frequently determined by the method of excitation and/or the physical boundaries of the specimen. Only specialized texts explore the mode of acoustic propagation in liquid-crystals. French (1971) provides a good bibliography of acoustic propagation but does not include more recent works such as Lighthill (1978), Main (with three similar editions through 1993) or Biryukov et al. (1995). Lighthill differentiates between surface acoustic waves of the gravity type and the surface tension type. The surface tension type of slow traveling waves (also called capillary waves) are the type of interest in the TM. Biryukov et al. is the current bible in the field of surface acoustic wave propagation in inhomogeneous materials. Oliner discusses the symmetric and antisymmetric forms of topographic waveguides and their Rayleigh wave velocity. He notes the symmetric, or Pseudo-Rayleigh, mode of a topographic waveguide (such as Hensen's stripe—whether rectangular or wedge shaped) exhibits propagation down to zero frequency and almost no dispersion with frequency. Both Lighthill and Biryukov et al. note the theoretically infinite space constant associated with surface acoustic waves under appropriate conditions.

**Figure M.2.3-1** shows the major modes of Rayleigh wave propagation on a thin coating of gold on a fused quartz substrate from Ohm & Hamilton<sup>13</sup>. The substrate is assumed to occupy a "half-space" (a hemisphere) in rheology jargon. The first mode, R1, approaches the Rayleigh velocity for a surface acoustic wave as the wavenumber,  $kh$ , increases. The Rayleigh velocity for a shear wave in the same material is typically only slightly higher than that for the surface acoustic wave.

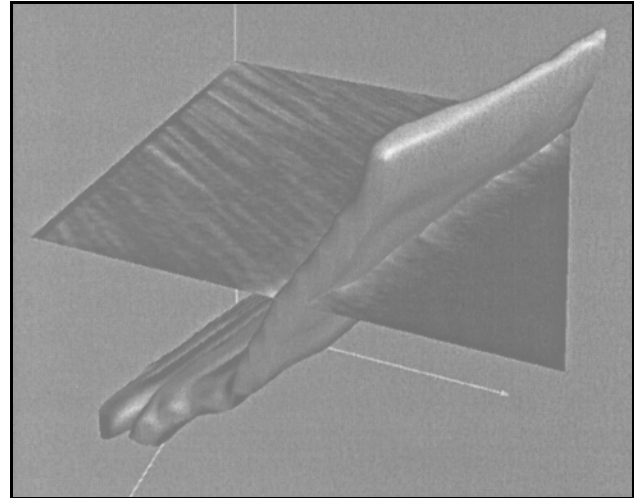


**Figure M.2.2-1** A surface rendered model of the shell-like structure (Kimura's membrane) between the bulk TM (to the left) and the endolymph (to the right). From Gueta et al., 2007

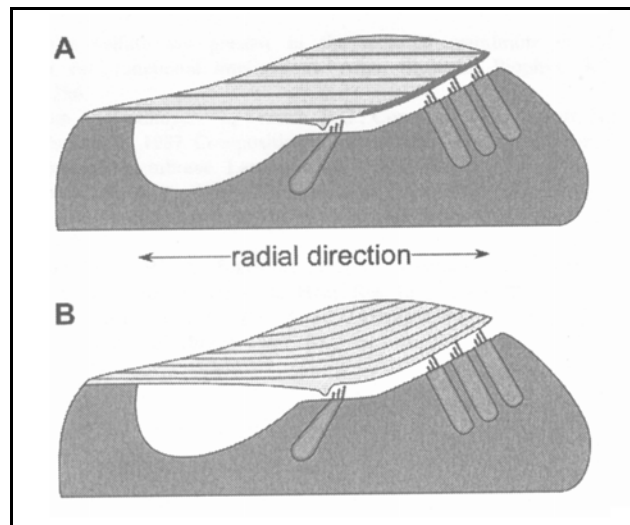


**Figure M.2.2-2** Schematic representation of the Organ of Corti showing arrangement of the collagen fibers in the TM. The "radial direction" is schematic and does not conform to the local radius of the curved cochlear partition or the orientation of the collagen fibers within the TM. From Gueta, Tal et al., 2007.

## 8 Hearing: A 21<sup>st</sup> Century Paradigm

The Rayleigh velocity is a function of the material and can be quite low. Ghaffari et al. have demonstrated that the closely related Lamb wave (based on their description) velocity of the shear wave in a liquid crystal/gas interface is less than 6 meters/second in the apical region of the bulk TM of the mouse. On average, it is less than 8 meters/second in the basal region. They fitted a line very similar to that of equation 52 of Lighthill to their data. They appear to fit the 10mm and 20 mm depth curves of water from figure 57 of Lighthill to their data points. Interestingly, the Lighthill equation is for sagittal ripples on a water/air interface and not the lateral waves associated with a Lamb wave.

Ohm & Hamilton also develop the concept of *stiffening dispersion* and *loading dispersion* depending on the ratio between the bulk wave velocities in the coating material and the bulk material. They assert only the first Rayleigh mode can exist in material where the bulk wave speed in the coating (scala media) exceeds that in the substrate material (liquid crystal) by more than the square root of two. This is certainly the case in the TM/scala media case.

The stiffening of the shell noted by Gueta, Tal et al. may be an optimization used in the development of the cochlear partition.

### M.2.3.1 Wave velocities at the immersed interface between two liquids

Main (1993) has provided a textbook presentation on the velocity of wave propagation at a liquid/air (air density negligible compared to the liquid) boundary. It is relatively brief. Lighthill (1978) has provided a more detailed discussion of the same mechanism at the same boundary. It is more complete but difficult to follow. Patuzzi developed the same material in 1996 (page 210-212) based on Main. However, his development is limited and the equations suffer from multiple typesetting errors.

These works do not address the actual interface between two liquid or liquid like materials. Their equations do not apply to an immersed interface.

Biryukov et al. (pp 11-13) address the surface acoustic waves (SAW) formed at an immersed interface, within a layered structure. The gravity term of the Lighthill and of the Main equations, as expressed in Patuzzi in 1996 and in Frosch at the 2008 Keele conference, drop out of the dispersion equation under this circumstance.

The dispersion equation for a shallow liquid becomes;

$\omega^2 = (g \cdot k + Tk^3/\rho)\tanh(h \cdot k)$	liquid/gas interface
$\omega^2 = (g \cdot k(1 - \rho_2/\rho_1) + Tk^3/\rho_1)\tanh(h \cdot k)$	liquid/liquid interface
$\omega^2 = (0 + Tk^3/\rho)\tanh(h \cdot k)$	$\rho_2 = \rho_1$ liquid/liquid interface

**Figure M.2.3-2** Dispersion relationships for various fluid/fluid interfaces. Top; a fluid-air interface subject to gravity. Middle; a liquid/liquid interface. Bottom, a liquid/liquid interface where the two liquids have the same density. The g-term drops out for an immersed interface between liquids of similar density..

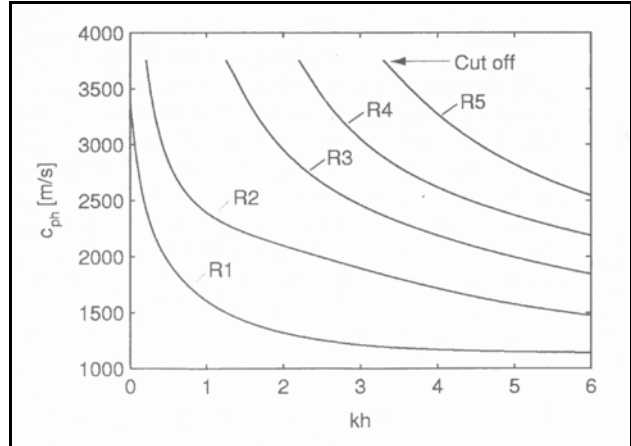


**Figure M.2.3-1** The Rayleigh modes of acoustic vibration in a polycrystalline gold coating on fused quartz. The first Rayleigh mode is designated R1. From Ohm & Hamilton, 2004.



where the term including  $g \cdot k$  is zero for an immersed interface between two liquids or a liquid and a gel of the same density ( $\rho$ ).

For an effectively deep interface, the term  $\tanh(k \cdot H)$  becomes equal to 1.00 and the equation is simplified further. Equating the average velocity of the SAW from the data of Ghaffari et al. with the equation for the liquid/liquid crystal interface, the value of T, the surface tension of the resulting structure is;

$$c = (T \cdot 2\rho / \rho \cdot \lambda)^{0.5} \approx 6 \text{ meters/sec}$$

Solving for T, an approximate value for T is

$$T \approx 5.7 \text{ kgms/sec}^2 = 5.7 \text{ Newtons/meter}$$

at 10 kHz It remains near this value down to at least 3 kHz in mice. This value is approximately 100 times the surface tension of pure water,  $T_{\text{water}} = 0.074 \text{ N/m}$  at 12 C, under static conditions even though the active surface material of the tectorial membrane is estimated to consist of 95% water and the scala media is essentially all water. This value clearly illustrates the difference between the dynamic surface tension at the interface compared to the static value.

## M.2.4 Parameters of surface acoustic waves in liquid crystals

As noted earlier, it is possible to achieve surface acoustic waves traveling along the surface between a liquid crystal and a second fluid medium with exceptional properties. The properties of such materials frequently result in what are called “ringing gels,” static materials that when excited can sustain energy oscillations between the boundaries of the container that have time constants on the order of seconds at frequencies in the audio range, typically around 1000 Hertz. Thus it takes more than 1000 cycles of the material for the energy to dissipate to 1/e of its initial density (compared to 10 cycles in many similar materials). Such durations suggest the quality factor, Q, for such a material is on the order of 3140, a very high value for any material (French, pgs 68 & 100).

The following relationships hold for a damped oscillating system:

Upon cessation of excitation in a simple oscillatory system, the amplitude of oscillation falls to 1/e after  $Q/\pi$  cycles.

$$Q = \omega_0 / \gamma = 2\pi f_0 / \gamma = \omega_0 \cdot m / b \qquad \gamma = b/m \qquad \omega_0^2 = k/m$$

where m is the mass of the system, b is the resistive component and k is the spring constant,  $\gamma$  is the damping coefficient, and  $\omega_0$  is the natural angular frequency of the system in the absence of damping.

For a surface acoustic wave traveling on such a material, the space constant can be expected to be on the order of 1000 wavelengths, or about 6 meters at 1000 Hertz and 6 meters/sec. Even if the 1000 cycles of the tone should represent three time constants, the space constant could be expected to be on the order of two meters. ***These space constants for the surface acoustic wave are exceedingly long compared to the 237 microns measured by Ghaffari et al for a bulk shear wave traveling at the same speed in an actual mouse TM.*** It appears compatible with the space constant observed in the guinea pig by Tasaki in 1952. It is also compatible with the theoretical model summarized in **Section M.1.1**.

Tasaki measured the amplitude of the electrical signal generated across the cochlear partition at three locations simultaneously in the guinea pig. His protocol called for adjusting the gain of the three measurement channels so the relative amplitudes of the actual signals were preserved. **Figure M.2.4-1** shows his unexpected results. The signal amplitude at frequencies below BF at a given location were not attenuated significantly when traveling the length of the cochlea to that location. At 200 Hertz, the signal traveled the majority of the length of the cochlear partition with negligible attenuation. The apical turn is on the order of 15-18 mm from the base of the cochlea in the guinea pig (**Section 4.5.4**). The only known means of achieving such performance is if the acoustic energy traverses the cochlear partition as a surface acoustic wave with a space constant several times the length of the cochlear partition. In the case of large animals, a space constant of at least tens of centimeters is to be expected.

## 10 Hearing: A 21<sup>st</sup> Century Paradigm

At frequencies slightly below BF, a small *increase* in amplitude was routinely recorded relative to earlier values along the partition (as reported elsewhere and predicted by the theory of this work, **Section 4.5.2**). Above BF, the attenuation was severe as also predicted in **Section 4.5.2** and measured routinely. Both the increase before BF and rapid decrease after BF are due to the Marcatili mechanism and the curvature of the cochlea.

Oetter & Hoffman provide an extensive discussion of liquid-crystalline materials from the rheology perspective<sup>14</sup>. They define a ringing gel as an optically isotropic microemulsion in a ternary system, surfactant, hydrocarbon and water with a typically liquid-crystalline cubic phase. They note that each of the components is in the liquid phase but the super-lattice is a solid. The Polymer & Liquid Crystal laboratory at Case Western Reserve University discusses this liquid-crystalline lattice in greater detail (<http://plc.cwru.edu/tutorial/enhanced/files/lc/phase/phase.htm>) **Figure M.2.4-2** illustrates the concept. The individual water molecules of the fluid matrix are much too small to be shown in this figure. Cases are known where the micelles are elongated and the resultant structure consists of lamellar pentagonal or hexagonal arrays<sup>15</sup>.

Oetter & Hoffmann note the energy storage is in the distortion of a lattice or an amorphous glass.” Such elements exhibit little friction loss. They note measuring the performance of these materials requires the use of a rheometer in the dynamic mode of operation, i. e., at the frequencies of interest..

The optical isotropism, and the general transparency, of these materials makes their imaging in visible light difficult. Thus, imaging Kimura’s membrane for measurement purposes is difficult. Special techniques, such as phase contrast microscopy, are frequently necessary to image the actual membrane. The second harmonic imaging microscope (SHIM) appears ideal for imaging the TM and its components.

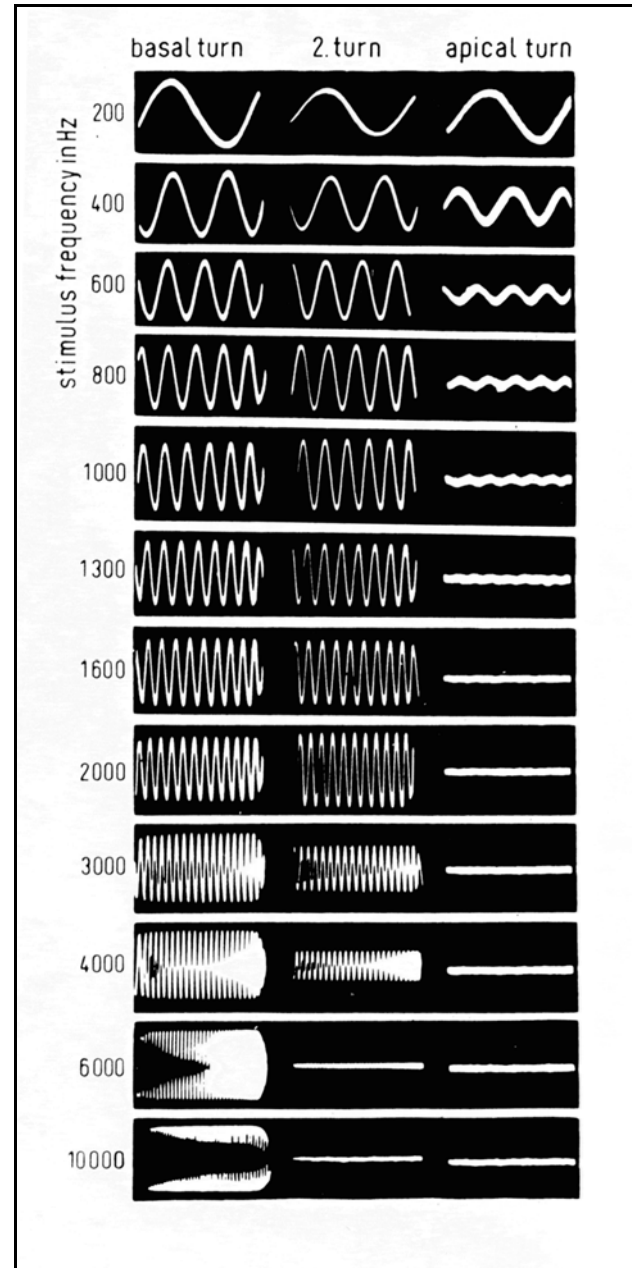


**Figure M.2.4-1** Relative amplitudes of electrical signals measured at three locations along the cochlear partition of the guinea pig. From Tasaki, 1952.

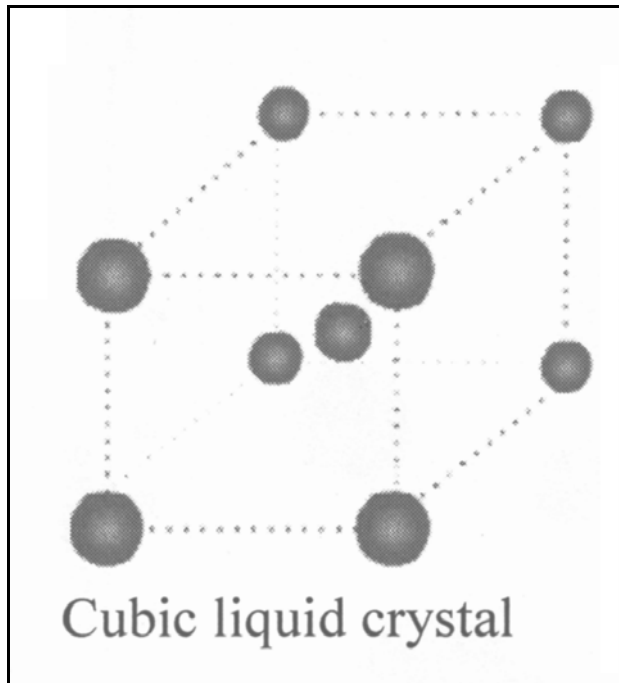


**Figure M.2.4-2** A body-centered cubic lattice of micelles of protein immersed in a water matrix. The water molecules are too small to show in this figure.

They also note the very low attenuation associated with these surface acoustic waves. Time constants exceeding one second are not uncommon. A time constant of one second suggests a significant signal over a distance of 1000 wavelengths for a frequency of 1000 Hz. Using Ghaffari et al.'s value of 4 meters/second at 10 kHz, the SAW traveling along the TM/scala media interface would exhibit negligible loss over the 35 mm length of the Organ of Corti. In practice, a 10 kHz wave only travels 5 mm within the OC.

### M.2.5 Acousto-mechanical model of TM

**Figure M.2.5-1** presents a theoretical model of the tectorial membrane beginning with the simplest presentation. The left frame shows a totally theoretical uniform density TM with a uniform density gel coating between the bulk TM and the uniform endolymphatic fluid. All dimensions of the model extend to infinity to eliminate any reflections of the energy introduced into the model at boundaries. The right frame shows two practical modifications of the theoretical model encountered in the real TM. First the semi-infinite substrate is truncated by an absorber of matching impedance that will not support the reflection of energy. This absorber is analogous to the covering net of the real TM. As long as the impedances are matched, it is not necessary for the covering net to be parallel to the gel coating. Second, the gel coating is truncated on the right by an absorber of matching

impedance that will not support the reflection of energy. This absorber is analogous to the marginal net of the real TM.

The coordinate system shown is arbitrary. There is no requirement that the energy, indicated by the vector  $k$ , flow parallel to the x-axis. In the real TM, there are lenticular fibrils (micelles) arranged near the surface of the substrate material that are believed to be parallel to the direction of energy flow. In the real TM, the x-axis is generally labeled the radial axis when examining small samples of the TM. Under those circumstances, the x-axis should be taken as perpendicular to the axis of the marginal net and the y-axis can be considered the longitudinal axis that is parallel to the marginal net.

In the theory presented in this work, the energy propagates across Kimura's membrane only in the positive x-direction due to the means by which the acoustic energy is introduced into the surface between the gel and the fluid (Marcatili's mechanism).

#### M.2.5.1 Protocols for exploring surface acoustic waves at the gel-fluid interface of the TM

**Sections M.2.4** and **M.2.5** have provided a framework for laboratory investigations of acoustic energy propagation on the gel-fluid interface of the TM. It should be clear that the gel-fluid interface can support a number of acoustic energy propagation modes and that uncontrolled boundaries can cause multiple reflections of these modes. The result can be a confusing set of intersecting waves propagating uncontrollably across the surface of the interface. Morse & Ingard illustrate a variety of these possibilities for a mechanical membrane (pages 206-216 of 1986 edition). With the extremely long space constants of the expected waves, the resulting wave patterns can exist for a very long time and result in standing wave patterns of great complexity. Efforts must be taken to minimize the number of propagating acoustic energy modes introduced into the test sample. It is also important to limit, or control, the uncontrolled reflections at the boundaries of the sample.

Ohm & Hamilton have discussed the propagation of Rayleigh waves in thin structures similar to the TM. They note (their figure 2 and accompanying text) that for thin coatings, where the wavelength of the propagated energy is much longer than the thickness of the coating, most of the higher order modes are suppressed and only the first Rayleigh mode need be considered. This appears to be the case in hearing.

It is important to note the following. If the model shown on the right is correct, the TM of hearing operates as an analog of a semi-infinite bulk material and not as a thin plate. It is important to develop any detailed mathematical

## 12 Hearing: A 21<sup>st</sup> Century Paradigm

model of the TM in accordance with whether it is a semi-infinite volume or a thin plate. The mathematics are quite different for the two cases.

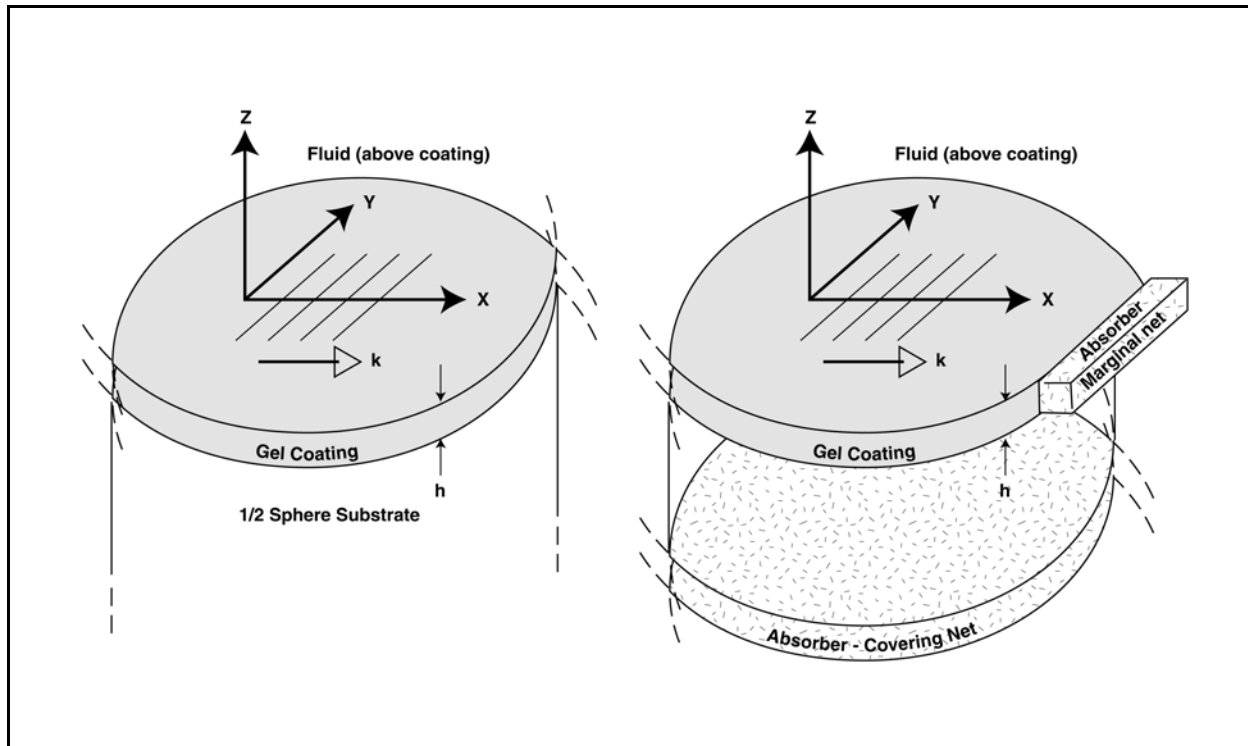


**Figure M.2.5-1** A theoretical acousto-mechanical model of the tectorial membrane. Left; the fundamental model of a gel coating on a semi-infinite substrate (a half-space) supporting the propagation of a surface acoustic wave at the gel-fluid interface. Right; a description of the real tectorial membrane with a real absorber of matching impedance, the covering net, replacing the semi-infinite substrate. An additional absorber of matching impedance, the marginal net, is shown replacing the infinite extent of the gel coating on the right side.

The predicted space constants are so large for the surface acoustic waves traveling on the gel-fluid surface of actual TM materials, it is difficult to measure them in small samples of actual TM material. It may be necessary to attempt the measurement on full longitudinal samples of the interface.

### M.2.6 Finite element modeling of the TM

The cochlear partition has been modeled using a variety of simple lumped constant models. However, the major components of the cochlear partition are clearly distributed structures with well known variations in their physical properties. The more sophisticated method of modeling this region is using finite element modeling techniques<sup>16</sup>. Finite element modeling (FEM) is a valuable tool for visualizing the dynamics of a structure in response to a specific mode of stimulation. However, the modeling process is highly dependent on the concept of the structure in the mind of the modeler. This section will develop several different outcomes from FEM applied to the TM and the TM/BM system.

FEM began in the 1960's as a method of modeling static structures. With the arrival of significant levels of computer power, it became possible to model dynamic structures as well. The complexity of the structures that could be handled increased directly with the available computer power and the length of time the modeler was willing to wait for the answer. The "bible" of FEM has been the multiple editions (now in multiple volumes) of Zienkiewicz & Taylor<sup>17</sup>. Recently, Lehmann has provided a volume on "Wave Propagation in Infinite Domains"<sup>18</sup>, but it appears to be limited to local bulk waves within structures. Neither of these works address surface acoustic waves along a boundary of a structure and the appropriate treatment of such a situation. Standard FEM techniques generally treat either external point loads or external spatially uniform loads applied to a dynamic structure. While superposition can be used to address more complex loadings, the modeling of a surface acoustic wave traveling along a TM membrane and intercepting a local load associated with the cilia of an OHC or IHC does not appear to

have been addressed using FEM techniques.

Finite element modeling of the TM has been undertaken on multiple occasions. It is important that the mathematical model used in this process reflect the actual acoustic properties (physical properties at the relevant frequencies) of the TM as well as its general physical properties. Specifically, the finite element model must reflect the heterogeneous character of the TM described in **Section M.1.1**. It must also reflect the variations in viscosity with frequency associated with a liquid-crystalline structure.

In addition, the FEM must employ realistic forces to excite the model. The appropriate excitation is strongly affected by the overall model of hearing assumed by the investigator. Baumgart et al. assumed the only forces applied to the FEM representing the cross-section of the cochlear partition were from the electrical motility of the soma of the three OHC and that the elasticity of the BM provided a resonance at the driving frequency of 0.8 kHz<sup>19</sup>. On the other hand, the reported motions of the BM in-vivo are due to two independent, and nearly simultaneous, points of excitation (**Sections 4.3.3.4, 4.6.3** & animation on the website [www.hearingresearch.net/files/animation.htm](http://www.hearingresearch.net/files/animation.htm)). These motions are the cause of the well documented Kiang's seam or notch.

In the absence of adequate modeling and appropriate excitation, the FEM may not reflect the actual physical motions of the TM and BM under realistic conditions. An appropriate FEM, appropriately excited, should reflect the actual movements of the cochlear partition. These movements should reflect the delay associated with the place-frequency-delay map, and not require major changes in the parameters of the model to create a resonant condition artificially.

### **M.3 Critical steps in the laboratory protocol**

The requirement to preserve the unique physical properties of the TM make its handling in the laboratory extremely demanding.

While the term membrane is used widely in the biological literature, it has an entirely different meaning in the world of mechanics. A biological membrane is generally not under tension, is not homogeneous and seldom forms a planar surface. It usually includes inclusions or out of plane features. In many cases, such as Kimura's membrane, the membrane is more effectively described as a coating. Neither the bulk of the TM or the BM are membranes in the world of mechanics.

While not commonplace at present, it is important to maintain the physical coordinates and orientation in its native state of each portion of the TM that is used in subsequent examination. This is a major requirement in similar fields such as field archeology and paleontology. Physical straightening of individual portions of the TM should be avoided as this process disturbs the functional relationship between the elements of the TM.

The liquid-crystalline character of much of the TM requires unique handling. The sensitivity of elements of the TM to solvation requires great care. Every effort must be made to avoid the introduction of detergents or sodium containing alkali compounds into the fluids in contact with the TM. The preferred procedure is to replace the perilymph of the cochlea with an artificial endolymph (or other non sodium bearing solution) before the scala media is opened. Similarly, the sensitivity of the elements of the TM to phase change requires the temperature of the specimen be maintained very close to homeostatic conditions. Temperatures above the Debye temperature and below freezing must be avoided as these boundaries relate to phase changes in the material.

# 14 Hearing: A 21<sup>st</sup> Century Paradigm

## Table of Contents

M.1 Introduction & Overview	1
M.1.1 Framework for subsequent discussion	3
M.1.1.1 Laboratory techniques of special interest	4
M.1.1.2 Terminology	4
M.2 Detailed description of the tectorial membrane	5
M.2.1 The physical properties of the <i>static</i> tectorial membrane ca. 2006	5
M.2.2 The 3D structure of the tectorial membrane in 2007	6
M.2.3 Modes of oscillation within, and on, the TM	7
M.2.3.1 Wave velocities at the immersed interface between two liquids	8
M.2.4 Parameters of surface acoustic waves in liquid crystals	9
M.2.5 Acousto-mechanical model of TM	11
M.2.5.1 Protocols for exploring surface acoustic waves at the gel-fluid interface of the TM	11
M.2.6 Finite element modeling of the TM	12
M.3 Critical steps in the laboratory protocol	13

## List of Figures

<b>Figure M.1.1-1</b> Cross section of the Organ of Corti taken as a gross reference	2
<b>Figure M.1.1-2</b> Proposed detail configuration of the vestibule and cochlear duct	3
<b>Figure M.2.1-1</b> A phase contrast transmitted light microscope image of a TM sample	5
<b>Figure M.2.2-1</b> A surface rendered model of the shell-like structure (Kimura's membrane)	7
<b>Figure M.2.2-2</b> Schematic representation of the Organ of Corti showing arrangement of the collagen	7
<b>Figure M.2.3-1</b> The Rayleigh modes of acoustic vibration in a polycrystalline gold coating	8
<b>Figure M.2.3-2</b> Dispersion relationships for various fluid/fluid interfaces	8
<b>Figure M.2.4-1</b> Relative amplitudes of electrical signals measured at three locations along the cochlear	10
<b>Figure M.2.4-2</b> A body-centered cubic lattice of micelles of protein immersed in a water	11
<b>Figure M.2.5-1</b> A theoretical acousto-mechanical model of the tectorial membrane	12

## SUBJECT INDEX (using advanced indexing option)

95%	1, 4, 9
average velocity	9
bilayer	6
caecum	2
curvature of Hensen's stripe	5
FEM	12, 13
half-space	7, 12
Hensen's stripe	3-6
homogeneous	5, 13
inhomogeneous	7
knockout	6
Lamb wave	8
Langmuir	6
launcher	2, 3
liquid-crystalline	1-7, 10, 13
Marcatili	3, 10
OHC	3, 4, 7, 12, 13
perilymph	6, 13
piezoelectric	4
place-frequency	13
place-frequency-delay	13
Rayleigh wave	7
Reissner's	5
resonance	13

reticular lamina .....	5
rheology .....	6, 7, 10
ringing .....	6, 9, 10
scala media .....	2, 5, 8, 9, 11, 13
seam .....	13
tectorial membrane .....	1-6, 9, 11, 12
topographic waveguides .....	7
tubulin .....	5
type B .....	6
vestibule .....	3

## 16 Hearing: A 21<sup>st</sup> Century Paradigm

1. Ghaffari, R. Aranyosi, A. & Freeman, D. (2007) Longitudinally propagating traveling waves on the mammalian tectorial membrane *PNAS*, vol 41, pp 16510-16515
2. Iurato, S. (1967) *Submicroscopic Structure of the Inner Ear*. NY: Pergamon Press pp 160-168
3. Kronester-Frei, A. (1978) Ultrastructure of the different zones of the tectorial membrane *Cell Tiss Res* vol. 193, pp 11-23
4. Kronester-Frei, A. (1979) The effect of changes in endolymphatic ion concentration on the tectorial membrane *Hear Res* vol.1, pp 81-94
5. Pack, A. Slepecky, N. (1995) Cytoskeletal and calcium-binding proteins in the mammalian organ of Corti: *Hear Res* vol. 91, pp 119-135
6. Harrison, R. & Hunter-Duvar, I. (1988) An anatomical tour of the cochlea *In* Jahn, A. & Santos-Sacchi, J. eds. *Physiology of the Ear*, 1<sup>st</sup> Ed. NY: Raven Press pp 159-172
7. Santi, P. (1988) Cochlear microanatomy and ultrastructure *In* Jahn, A. & Santos-Sacchi, J. eds. *Physiology of the Ear*, 1<sup>st</sup> Ed. NY: Raven Press pp 173-199
8. Novoselova, S. (2003) Notes on physical properties of the tectorial membrane *In* Gummer, A. ed. *Biophysics of the Cochlea*. Singapore: World Scientific pp 368-392
9. Masaki, K. Freeman, D. Richardson, G. & Smith, R. (2006) Comparing the equilibrium stress-strain relations of tectorial membranes from *Tecta* Y1870C and *Col11a2* <sup>-/-</sup> mouse mutants *In* Nuttall, A. et. al. eds. *Auditory Mechanisms: Processes and Models*. Singapore: World Scientific pp 49-55
10. Cotanche, D. & Corwin, J. (1990) Stereociliary bundles reorient during hair cell development and regeneration in the chick cochlea *Hear Res* vol 52, pp 379-402, pg 399
11. Radiman, S. Toprakcioglu, C. & McLeish, T. (1994) Rheological study of ternary cubic phases *Langmuir* Vol.10, pp 61-67
12. Gueta, R. Tal, E. Silberberg, Y. & Rousso, I. (2007) The 3D structure of the tectorial membrane determined by second-harmonic imaging microscopy *J Struct Biol* vol 159, pp 103-110
13. Ohm, W-S. & Hamilton, M. (2004) Evolution of nonlinear Rayleigh waves in a coated substrate *J Acoust Soc Am* vol 115(6), pp 2798-2806
14. Oetter, G. & Hoffmann, H. (1989) Ringing gels and their fascinating properties. *Colloids Surf* vol 38, pp 225-250
15. Lieberman, H. Rieger, M. & Banker, G. (1996) *Pharmaceutical dosage forms: disperse systems*, 2<sup>nd</sup> Ed. vol 3. NY: Dekker pg 19
16. Zienkiewicz, O. Taylor, R. & Zhu, J. (2006) *The Finite Element Method*. NY: Elsevier
17. Zienkiewicz, O. & Taylor, R. (1989) *The Finite Element Method*, 4<sup>th</sup> Ed, Volumes 1 & 2. NY: McGraw-Hill
18. Lehmann, L. (2007) *Wave Propagation in Infinite Domains*. NY: Springer
19. Baumgart, J. Chiaradia, C. Fleischer, M. et al. (2009) Fluid mechanics in the subtectorial space *In* Cooper, N. & Kemp, D. ed. *Concepts and Challenges in the Biophysics of Hearing*. Singapore, World Scientific